International Journal of
Science and Engineering Investigations vol. 8, issue 92, September 2019
Received on August 28, 2019 ISSN: 2251-8843

Chemically Reacting Ionized Fluid Flow through a Porous Medium along an Impulsively Started Permeable Vertical Plate with Induced Magnetic Field and Viscous Dissipation

Tanvir Ahmed[1], Md. Mahmud Alam[2], M. Z. I. Bangalee[3], M. Ferdows[4], Raushan Ara Quadir[5]
[1,2]Mathematics Discipline, Khulna University, Khulna 9208, Bangladesh
[3,4]Research Group of fluid flow modeling and simulation, Department of Applied Mathematics, University of Dhaka, Dhaka-1000, Bangladesh
[5]School of Mathematics, Statistics and Computer Science, University of KwaZulu Natal, South Africa
([4]ferdows@du.ac.bd)

Abstract- The numerical simulations of the chemically reacted ionized fluid flow through a vertical plate with induced magnetic field have been performed for cooling problem. To obtain the non-dimensional non-similar momentum, induced magnetic field, energy and concentration equations, usual non-dimensional variables have been used. The obtained non-dimensional, coupled partial differential equations have been solved by finite difference method. The effects of the various parameters entering into the problem on the shear stresses, current densities, Nusselt number and Sherwood number are discussed in graphical form. Also the stability conditions of the finite difference method are investigated. Finally, a qualitative comparison of the present results with previous published results has been shown.

Keywords-*Ionized Fluid, Induced Magnetic Field, Viscous Dissipation, Chemical Reaction, Soret and Dufour Effect, Finite Difference Method*

I. INTRODUCTION

The study of ionized fluid flow on boundary layer flow has become important in several industrial processes, scientific and engineering fields. It has been considered by Cowling [1] that the ionized fluid has two distinct effects. The convection flow is often encountered in nuclear reactors or in the study of planets and stars. There are many engineering problems are susceptible to ionized fluid flow analysis. It is useful in astrophysics because much of the universe is filled with widely spaced charged particles and permeated by magnetic fields and so the continuum assumption becomes applicable. In many engineering applications, combined heat and mass transfer play an important role in fluids condensing or boiling at solid surface. Studies of MHD incompressible viscous flows with Hall currents have grown considerably because of its engineering applications to the problems of Hall accelerators, MHD generators, constructions of turbines and centrifugal machines, as well as flight magnetohydrodynamics. The effects of Hall currents on free convective flow through a porous medium bounded by an infinite vertical plate have been studied by Ram [2], when a strong magnetic field is imposed in a direction which is perpendicular to the free stream and makes an angle to the vertical direction. Combined effects of thermal radiations and Hall current on moving vertical porous plate in a rotating system with variable temperature have been analyzed by Garg [3]. The interaction of buoyancy with thermal radiation has been increased greatly during the last decade due to its importance in many practical applications. The similarity analysis of magnetic field and thermal radiation effects on forced convection flow have been investigated by DAMSEH et al. [4]. The effect of thermal radiation interaction with unsteady MHD flow past a vertical porous plate immersed in a porous medium has been studied by Samad and Rahman [5].

The growing need for chemical reactions in chemical and hydrometallurgical industries requires the study of heat and mass transfer with chemical reaction. There are many transport processes that are governed by the combined action of buoyancy forces due to both thermal and mass diffusion in the presence of the chemical reaction. The effect of the first-order homogeneous chemical reaction of an unsteady flow past a vertical plate with the constant heat and mass transfer has been investigated by Das et al. [6]. The MHD mixed convection interaction with thermal radiation and nth order chemical reaction past a vertical porous plate embedded in a porous medium have been studied by Makinde [7]. The heat and mass transfer occur simultaneously between the fluxes; the driving potentials are of more intricate nature. An energy flux can be generated not only by temperature gradients but by composition gradients. The energy flux caused by a composition is called Dufour or diffusion-thermo effect. Temperature gradients can also create mass fluxes, and this is the Soret or thermal-diffusion effect. The boundary layer-flows in the presence of Soret and Dufour effects associated with the thermal diffusion and diffusion-thermo for the mixed convection have been analyzed by Kafoussias and Williams [8]. The influence of a magnetic field on heat and mass transfer by natural convection from vertical surfaces in porous media considering Soret and Dufour effects have been studied by Postelnicu [9]. The effect of thermal radiation, Hall currents, Soret and Dufour on MHD flow by mixed convection over a

vertical surface in porous media has been studied by Shateyi et al. [10]. The effects of Soret, Dufour, chemical reaction, thermal radiation and volumetric heat generation/absorption on mixed convection stagnation point flow on an isothermal vertical plate in porous media has been analyzed by Olanrewaju and Gbadeyan [11]. Recently, the effects of Soret and Dufour on unsteady MHD flow by mixed convection over a vertical surface in porous media with internal heat generation, chemical reaction and Hall current has been investigated by Aurangzaib and Shafie [12]. Ahmed and Alam [13] solved the Aurangzaib and Shafie [12]'s model by finite difference method.

The above papers cited earlier, the studies concentrated aon MHD free convection heat and mass transfer flow of an incompressible viscous fluid past a continuously moving surface under only the action of transverse magnetic field with or without thermal diffusion, diffusion thermo and chemical reaction for small Magnetic Reynolds number. If the Magnetic Reynolds number of the flow is not taken to be small enough that induced another magnetic field has of great interest in fluid dynamics. The unsteady heat and mass transfer by mixed convection flow from a vertical porous plate with induced magnetic field, constant heat and mass flaxes has been investigated by Alam et al. [14].

The numerical study of Soret and Dufour effects on MHD free convective heat and mass transfer unsteady high speed flow of viscous fluid through a porous medium with induced magnetic field in a rotating system is investigated by Haque et al. [15]. For unsteady two dimensional cas, with Hall effect, chemical reaction, thermal radiation, thermal-diffusion, diffusion thermo, induced magnetic field and inclined uniform magnetic field the above problem becomes more complicated. These types of problems play a special role in nature, in many separation processes as isotope separation, in mixtures between gasses, in many industrial applications as solidification of binary alloy as well as in astrophysical and geophysical engineering.

Hence our aim of this work is to extend the work of Ahmed and Alam [13] with induced magnetic field. The problem has been solved by finite difference method [16]. The governing equations involved in this problem have been transformed into dimensionless non-similar coupled partial differential equation by usual transformations. Finally, the comparison of the present results with the results of Haque et al. [15] has been shown.

II. MATHEMATICAL MODEL OF THE FLOW

An unsteady chemically reacting ionized mixed convective heat and mass transfer flow of an electrically conducting incompressible viscous fluid through a porous medium along electrically nonconducting isothermal infinite vertical porous plate with thermal diffusion, diffusion thermo, joule heating and viscous dissipation effects are considered. The positive x coordinate is measured along the plate in the direction of fluid motion and the positive y coordinate is measured normal to the plate. The leading edge of the plate is taken as coincident with $z-$axis. Initially, it is considered that the plate as well as the fluid is at the same temperature $T(=T_\infty)$ and concentration $C(=C_\infty)$. Also it is assumed that the fluid and the plate is at rest after that the plate is to be moving with a constant velocity U_∞ in its own plane. Instantaneously at time $t>0$, the temperature of the plate and spices concentration are raised to $T_w(>T_\infty)$ and $C_w(>C_\infty)$ respectively, which are there after maintained constant, where T_w , C_w are temperature and spices concentration at the wall and T_∞, C_∞ are the temperature and concentration of the species outside the plate respectively. The physical configuration of the problem is furnished in Figure 1.

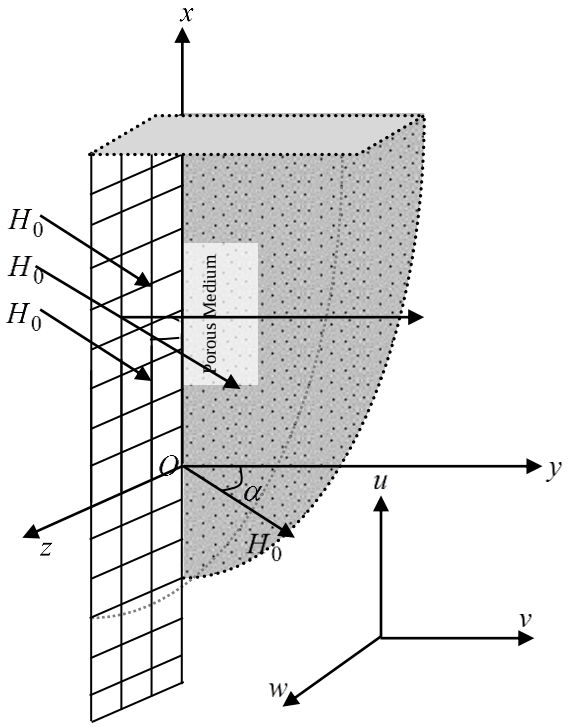

Figure 1. Geometrical configuration and coordinate system.

A strong uniform magnetic field H_0 can be taken as $(0, \lambda H_0, \sqrt{1-\lambda^2}H_0)$ where $\lambda = \cos\alpha$ is applied in a direction that makes an angle α with the normal to the considered plate. Thus if $\lambda = 1$ the imposed magnetic field is parallel to the $y-$axis and if $\lambda = 0$ then the magnetic field is parallel to the plate. The magnetic Reynolds number of the flow is not taken to be small enough; therefore the induced magnetic field is not negligible. The resultant magnetic field is of the form

$H = (H_x, H_y + \lambda H_0, H_y + \sqrt{1-\lambda^2}H_0)$. Using the relation $\nabla \cdot J = 0$ for the current density $J = (J_x, J_y, J_z)$ where $J_y =$ constant. Since the plate is nonconducting, $J_y = 0$ at the plate and hence zero everywhere. And the divergence equation

$\nabla \cdot H = 0$ of Maxwell's equation for the magnetic field gives $H_y = 0$. If the plate is infinite in extent and hence all physical quantities depend on *y* and *t.* Thus under the electromagnetic Boussinesq approximations, the MHD unsteady flow and heat and mass transfer with heat generation and chemical reaction are governed by the following equations are given by:

$$\frac{\partial v}{\partial y} = 0 \tag{1}$$

Momentum equations;

$$\frac{\partial u}{\partial t} - v_0 \frac{\partial u}{\partial y} = \upsilon \frac{\partial^2 u}{\partial y^2} + g\beta_T \left(T - T_\infty\right)$$

$$+ g\beta_C \left(C - C_\infty\right) - \frac{\mu}{\rho k_1} u + \frac{\mu_e \lambda H_0}{4\pi\rho} \frac{\partial H_x}{\partial y} \tag{2}$$

$$\frac{\partial w}{\partial t} - v_0 \frac{\partial w}{\partial y} = \upsilon \frac{\partial^2 w}{\partial y^2} - \frac{\mu}{\rho k_1} w + \frac{\mu_e \lambda H_0}{4\pi\rho} \frac{\partial H_z}{\partial y} \tag{3}$$

Magnetic induction equations;

$$\frac{\partial H_x}{\partial t} - v_0 \frac{\partial H_x}{\partial y} = \eta \frac{\partial^2 H_x}{\partial y^2} + \lambda H_0 \frac{\partial u}{\partial y} - \eta\lambda\beta_e \frac{\partial^2 H_z}{\partial y^2} \tag{4}$$

$$\frac{\partial H_z}{\partial t} - v_0 \frac{\partial H_z}{\partial y} = \eta \frac{\partial^2 H_z}{\partial y^2} + \lambda H_0 \frac{\partial w}{\partial y} + \eta\lambda\beta_e \frac{\partial^2 H_x}{\partial y^2} \tag{5}$$

Energy equation;

$$\frac{\partial T}{\partial t} - v_0 \frac{\partial T}{\partial y} = \frac{\kappa}{\rho c_p} \frac{\partial^2 T}{\partial y^2} + \frac{D k_t}{c_s c_p} \frac{\partial^2 C}{\partial y^2}$$

$$+ \frac{1}{16\pi^2 \rho c_p \sigma} \left(\left(\frac{\partial H_z}{\partial y} \right)^2 + \left(\frac{\partial H_x}{\partial y} \right)^2 \right)$$

$$+ \frac{\upsilon}{c_p} \left(\left(\frac{\partial u}{\partial y} \right)^2 + \left(\frac{\partial w}{\partial y} \right)^2 \right) - \frac{1}{\rho c_p} \frac{\partial q_r}{\partial y} + \frac{Q}{\rho c_p} \left(T - T_\infty\right)^p \tag{6}$$

Concentration equation;

$$\frac{\partial C}{\partial t} - v_0 \frac{\partial C}{\partial y} = D \frac{\partial^2 C}{\partial y^2} + \frac{D k_t}{T_m} \frac{\partial^2 T}{\partial y^2} - k_0 \left(C - C_\infty\right)^q \tag{7}$$

The corresponding boundary conditions for the problem are;

$$\left.\begin{array}{l} u = U_\infty,\ w = 0,\ H_x = H_w,\ H_z = 0, \\ T = T_w,\ C = C_w \text{ at } y = 0 \\ u = 0,\ w = 0,\ H_x = 0,\ H_z = 0, \\ T \to 0,\ C \to 0 \text{ as } y \to \infty \end{array}\right\} \tag{8}$$

where u and w are the x and z components of velocity vector, v_0 is the suction velocity, H_x and H_z are the x and z components of magnetic induction vector, H_w be the magnetic induction at the wall, H_0 is the constant magnetic field, g is the local acceleration due to gravity, β_T is the thermal expansion coefficient, β_C is the concentration expansion coefficient, υ is the kinematic coefficient viscosity, μ is the fluid viscosity, μ_e is the magnetic permeability, ρ is the density of the fluid, κ is the thermal conductivity, c_p is the specific heat at the constant pressure , k_0 is the rate of chemical reaction and D is the coefficient of mass diffusivity, k_t is the thermal diffusion ratio, c_s is the concentration susceptibility, respectively. Here p and q are considered as positive constant. The radiative heat flux q_r is described by the Rosseland approximation [17] such that $q_r = -\frac{4\sigma^*}{3k^*} \frac{\partial T^4}{\partial y}$, where σ^* and k^* are the Stefan-Boltzman constant and the mean absorption coefficient, respectively. If the temperature difference within the flow are sufficiently small so that the T^4 can be expressed as a linear function after using Taylor series to expand T^4 about the free stream temperature T_∞ and neglecting higher-order terms. This result in the following approximation: $T^4 \approx 4T_\infty^3 T - 3T_\infty^4$.

III. MATHEMATICAL FORMULATION

Since the solution of the governing equations (1-7) under the boundary conditions (8) will be based on the finite difference method, it is required to make the equations dimensionless. For this purpose, the following dimensionless quantities are introduced as;

$$Y = \frac{yU_\infty}{\upsilon},\ U = \frac{u}{U_\infty},\ W = \frac{w}{U_\infty},\ \tau = \frac{tU_\infty^2}{\upsilon},\ H_1 = \sqrt{\frac{\mu_e}{\rho}} \frac{H_x}{U_\infty},$$

$$H_3 = \sqrt{\frac{\mu_e}{\rho}} \frac{H_z}{U_\infty},\ \bar{T} = \frac{T - T_\infty}{T_w - T_\infty} \text{ and } \bar{C} = \frac{C - C_\infty}{C_w - C_\infty}$$

Using these relations, the following relations into the equations (2-7) and corresponding boundary conditions (8) after simplification, the following nonlinear-coupled partial differential equations in terms of dimensionless variables

$$\frac{\partial U}{\partial \tau} - S \frac{\partial U}{\partial Y} = \frac{\partial^2 U}{\partial Y^2} + G_r \bar{T} + G_m \bar{C} - KU + \lambda M \frac{\partial H_1}{\partial Y} \tag{9}$$

$$\frac{\partial W}{\partial \tau} - S \frac{\partial W}{\partial Y} = \frac{\partial^2 W}{\partial Y^2} - KW + \lambda M \frac{\partial H_3}{\partial Y} \tag{10}$$

$$\frac{\partial H_1}{\partial \tau} - S \frac{\partial H_1}{\partial Y} = \frac{1}{P_m} \frac{\partial^2 H_1}{\partial Y^2} + \lambda M \frac{\partial U}{\partial Y} - \frac{\lambda\beta_e}{P_m} \frac{\partial^2 H_3}{\partial Y^2} \tag{11}$$

$$\frac{\partial H_3}{\partial \tau} - S \frac{\partial H_3}{\partial Y} = \frac{1}{P_m} \frac{\partial^2 H_3}{\partial Y^2} + \lambda M \frac{\partial W}{\partial Y} + \frac{\lambda\beta_e}{P_m} \frac{\partial^2 H_1}{\partial Y^2} \tag{12}$$

$$\frac{\partial \bar{T}}{\partial \tau} - S\frac{\partial \bar{T}}{\partial Y} = \left(\frac{1+R}{P_r}\right)\frac{\partial^2 \bar{T}}{\partial y^2} + D_u\frac{\partial^2 \bar{C}}{\partial y^2} + E_c\left(\left(\frac{\partial U}{\partial Y}\right)^2 + \left(\frac{\partial W}{\partial Y}\right)^2\right)$$

$$+\frac{E_c}{4\pi P_m}\left(\left(\frac{\partial H_3}{\partial Y}\right)^2 + \left(\frac{\partial H_1}{\partial Y}\right)^2\right) + \beta\bar{T}^p \qquad (13)$$

$$\frac{\partial \bar{C}}{\partial \tau} - S\frac{\partial \bar{C}}{\partial Y} = \frac{1}{S_c}\frac{\partial^2 \bar{C}}{\partial Y^2} + S_r\frac{\partial^2 T}{\partial Y^2} - \gamma\bar{C}^q \qquad (14)$$

The dimensionless boundary conditions are;

$$\left.\begin{array}{l} U=1,\ V=0,\ W=0,\ H_1=\sqrt{\dfrac{\mu_e}{\rho}}\dfrac{H_w}{U_\infty} \\ =1(\text{say}),\ H_3=0,\ \bar{T}=1,\ \bar{C}=1 \text{ at } Y=0 \\ U=0,\ V=0,\ W=0,\ H_1=0,\ H_3=0, \\ \bar{T}\to 0,\ \bar{C}\to 0 \text{ as } Y\to\infty \end{array}\right\} \qquad (15)$$

where τ represents the dimensionless time, Y be the dimensionless Cartesian coordinates, U and W are the dimensionless velocity components, H_1 and H_2 are the dimensionless primary and secondary induced magnetic field, $\bar{T}$ is the dimensionless temperature, $\bar{C}$ is the dimensionless concentration, $S=\frac{v_0}{U_\infty}$ (Suction Parameter), $G_r=\frac{gB_T\left(T_w-T_\infty\right)\upsilon}{U_\infty^3}$ (Grashof Number), $G_m=\frac{gB_C\left(C_w-C_\infty\right)\upsilon}{U_\infty^3}$ (Modified Grashof Number), $K=\frac{\mu\upsilon}{\rho k_1 U_\infty^2}$ (Permeability of the porous medium), $M=\frac{1}{4\pi}\frac{H_0}{U_\infty}\sqrt{\frac{\mu_e}{\rho}}$ (Magnetic Parameter), $P_m=4\pi\sigma\upsilon\mu_e$ (Magnetic diffusivity Number), $R=\frac{16\sigma^* T_\infty^3}{3k^*\kappa}$ (Radiation Parameter), $P_r=\frac{\rho c_p\upsilon}{\kappa}$ (Prandtl Number), $D_u=\frac{Dk_t}{\upsilon c_s c_p}\frac{\left(C_w-C_\infty\right)}{\left(T_w-T_\infty\right)}$ (Dufour Number), $E_c=\frac{U_\infty^2}{c_p\left(T_w-T_\infty\right)}$ (Eckert Number), $\beta=\frac{Q\upsilon\left(T_w-T_\infty\right)^{p-1}}{\rho c_p U_\infty^2}$ (Heat Generation or Absorption Parameter), $S_c=\frac{\upsilon}{D}$ (Schmidt Number), $S_r=\frac{Dk_T}{\upsilon T_m}\frac{\left(T_w-T_\infty\right)}{\left(C_w-C_\infty\right)}$ (Soret Number) and $\gamma=\frac{k_0\upsilon\left(C_w-C_\infty\right)^{q-1}}{U_\infty^2}$ (Chemical Reaction Parameter).

IV. SHEAR STRESS, CURRENT DENSITY, NUSSELT AND SHERWOOD NUMBER

The quantities of chief physical interest are shear stress, current density, Nusselt number and Sherwood number. The following equations represent the shear stress at the plate, shear stress in x-direction, $\tau_x=\mu_0\left(\frac{\partial u}{\partial y}\right)_{y=0}$ which is proportional to $\left(\frac{\partial U}{\partial Y}\right)_{Y=0}$. The shear stress in z-direction, $\tau_z=\mu_0\left(\frac{\partial w}{\partial y}\right)_{y=0}$ which is proportional to $\left(\frac{\partial W}{\partial Y}\right)_{Y=0}$. From the induced magnetic field, the effects of various parameters on the current density have been investigated. The following equations represent the current density at the plate, current density in x-direction, $j_x=\mu_0\left(-\frac{\partial H_x}{\partial y}\right)_{y=0}$ which is proportional to $\left(-\frac{\partial H_1}{\partial Y}\right)_{Y=0}$. The current density in z-direction, $j_z=\mu_0\left(-\frac{\partial H_z}{\partial y}\right)_{y=0}$ which is proportional to $\left(-\frac{\partial H_3}{\partial Y}\right)_{Y=0}$. From the temperature field, the effects of various parameters on the local and average heat transfer coefficients have been studied. The following equations represent the heat transfer rate that is well known Nusselt number, Nusselt number, $N_u=-\mu_0\left(\frac{\partial T}{\partial y}\right)_{y=0}$ which is proportional to $-\left(\frac{\partial \bar{T}}{\partial Y}\right)_{Y=0}$. And from the concentration field, the effects of various parameters on the mass transfer coefficients have been analyzed. The following equations represent the mass transfer rate that is well known Sherwood number, Sherwood number, $S_h=-\mu_0\left(\frac{\partial C}{\partial y}\right)_{y=0}$ which is proportional to $-\left(\frac{\partial \bar{C}}{\partial Y}\right)_{Y=0}$.

V. NUMERICAL SOLUTIONS

For solving the non-dimensional system by the finite difference method, it is required a set of finite difference equation. In this case, the region within the boundary layer is divided by some perpendicular lines of Y-axis, where Y-axis is normal to the medium as shown in Figure 2. It is assumed that the maximum length of boundary layer is $Y_{\max}=(25)$ as corresponds to $Y\to\infty$ i.e. Y varies from 0 to 25 and the number of grid spacing in Y directions is $\bar{p}(=400)$, hence the constant mesh size along Y axis becomes $\Delta Y=0.0625(0\le Y\le 25)$ with a smaller time-step $\Delta t=0.001$.

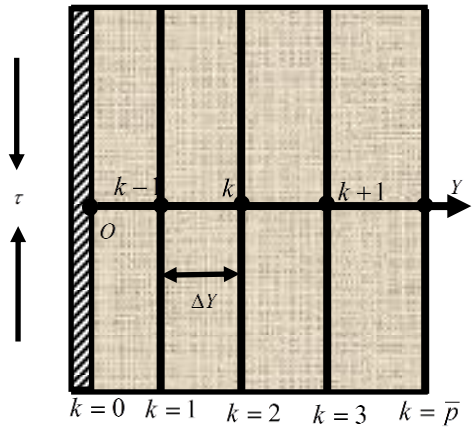

Figure 2. Finite difference system grid.

Let $U^{\bar{n}}, W^{\bar{n}}, H_1^{\bar{n}}, H_3^{\bar{n}}, \bar{T}^{\bar{n}}$ and $\bar{C}^{\bar{n}}$ denote the values of $U, W, H_1, H_3\ \bar{T}$ and $\bar{C}$ at the end of a time-step respectively. Using the finite difference approximation, the system of partial differential equations (9-14) and the boundary conditions (15), we obtain an appropriate set of finite difference equations,

$$\frac{U_k^{\bar{n}+1}-U_k^{\bar{n}}}{\Delta\tau}-S\frac{U_{k+1}^{\bar{n}}-U_k^{\bar{n}}}{\Delta Y}=$$

$$\frac{U_{k+1}^{\bar{n}}-2U_k^{\bar{n}}+U_{k-1}^{\bar{n}}}{(\Delta Y)^2}+G_r\bar{T}_k^{\bar{n}}+G_m\bar{C}_k^{\bar{n}} \tag{16}$$

$$\frac{W_k^{\bar{n}+1}-W_k^{\bar{n}}}{\Delta\tau}-S\frac{W_{k+1}^{\bar{n}}-W_k^{\bar{n}}}{\Delta Y}=\frac{W_{k+1}^{\bar{n}}-2W_k^{\bar{n}}+W_{k-1}^{\bar{n}}}{(\Delta Y)^2}-KW_k^{\bar{n}}$$

$$+\lambda M\frac{H_{3k+1}^{\bar{n}}-H_{3k}^{\bar{n}}}{\Delta Y} \tag{17}$$

$$\frac{H_{1k}^{\bar{n}+1}-H_{1k}^{\bar{n}}}{\Delta\tau}-S\frac{H_{1k+1}^{\bar{n}}-H_{1k}^{\bar{n}}}{\Delta Y}=$$

$$\frac{1}{P_m}\frac{H_{1k+1}^{\bar{n}}-2H_{1k}^{\bar{n}}+H_{1k-1}^{\bar{n}}}{(\Delta Y)^2}+\lambda M\frac{U_{k+1}^{\bar{n}}-U_k^{\bar{n}}}{\Delta Y}$$

$$-\frac{\lambda\beta_e}{P_m}\frac{H_{3k+1}^{\bar{n}}-2H_{3k}^{\bar{n}}+H_{3k-1}^{\bar{n}}}{(\Delta Y)^2} \tag{18}$$

$$\frac{H_{3k}^{\bar{n}+1}-H_{3k}^{\bar{n}}}{\Delta\tau}-S\frac{H_{3k+1}^{\bar{n}}-H_{3k}^{\bar{n}}}{\Delta Y}=$$

$$\frac{1}{P_m}\frac{H_{3k+1}^{\bar{n}}-2H_{3k}^{\bar{n}}+H_{3k-1}^{\bar{n}}}{(\Delta Y)^2}+\lambda M\frac{W_{k+1}^{\bar{n}}-W_k^{\bar{n}}}{\Delta Y}$$

$$+\frac{\lambda\beta_e}{P_m}\frac{H_{1k+1}^{\bar{n}}-2H_{1k}^{\bar{n}}+H_{1k-1}^{\bar{n}}}{(\Delta Y)^2} \tag{19}$$

$$\frac{\bar{T}_k^{\bar{n}+1}-\bar{T}_k^{\bar{n}}}{\Delta\tau}-S\frac{\bar{T}_{k+1}^{\bar{n}}-\bar{T}_k^{\bar{n}}}{\Delta Y}=+\beta\left(\bar{T}_k^{\bar{n}}\right)^p$$

$$\left(\frac{1+R}{P_r}\right)\frac{\bar{T}_{k+1}^{\bar{n}}-2\bar{T}_{ki}^{\bar{n}}+\bar{T}_{k-1}^{\bar{n}}}{(\Delta Y)^2}+D_u\frac{\bar{C}_{k+1}^{\bar{n}}-2\bar{C}_k^{\bar{n}}+\bar{C}_{k-1}^{\bar{n}}}{(\Delta Y)^2}$$

$$+\frac{E_c}{P_m}\left(\left(\frac{H_{3k+1}^{\bar{n}}-H_{3k}^{\bar{n}}}{\Delta Y}\right)^2+\left(\frac{H_{1k+1}^{\bar{n}}-H_{1k}^{\bar{n}}}{\Delta Y}\right)^2\right)$$

$$+E_c\left(\left(\frac{U_{k+1}^{\bar{n}}-U_k^{\bar{n}}}{\Delta Y}\right)^2+\left(\frac{W_{k+1}^{\bar{n}}-W_k^{\bar{n}}}{\Delta Y}\right)^2\right) \tag{20}$$

$$\frac{\bar{C}_k^{\bar{n}+1}-\bar{C}_k^{\bar{n}}}{\Delta\tau}-S\frac{\bar{C}_{k+1}^{\bar{n}}-\bar{C}_k^{\bar{n}}}{\Delta Y}=-\gamma\left(\bar{C}_k^{\bar{n}}\right)^q+$$

$$\frac{1}{S_c}\frac{\bar{C}_{k+1}^{\bar{n}}-2\bar{C}_k^{\bar{n}}+\bar{C}_{k-1}^{\bar{n}}}{(\Delta Y)^2}+S_r\frac{\bar{T}_{k+1}^{\bar{n}}-2\bar{T}_k^{\bar{n}}+\bar{T}_{k-1}^{\bar{n}}}{(\Delta Y)^2} \tag{21}$$

with the corresponding boundary conditions,

$$\left.\begin{aligned}&U_0^{\bar{n}}=1, W_0^{\bar{n}}=0,\ H_{10}^{\bar{n}}=1,\ H_{30}^{\bar{n}}=0,\\&\bar{T}_0^{\bar{n}}=1,\ \bar{C}_0^{\bar{n}}=1\\&U_L^{\bar{n}}=0, W_L^{\bar{n}}=0,\ H_{10}^{\bar{n}}=0,\ H_{30}^{\bar{n}}=0,\\&\bar{T}_L^{\bar{n}}=0, \bar{C}_L^{\bar{n}}=0\ \textit{where}\ \ L\to\infty\end{aligned}\right\} \tag{22}$$

Here the subscript k designates the grid points with Y coordinate and the superscript $\bar{n}$ represents a value of time, $\tau=\bar{n}\Delta\tau$ where $\bar{n}=0,1,2,\ldots\ldots$. The primary velocity (U), secondary velocity (W), primary induced magnetic field (H_1), secondary induced magnetic field (H_3), temperature $(\bar{T})$ and concentration $(\bar{C})$ distributions at all interior nodal points may be computed by successive applications of the above finite difference equations. The numerical values of the shear stresses, Current density, Nusselt number and Sherwood number are evaluated by Five-point approximate formula for the derivatives. The obtained values are graphically shown in Figures 3-14. The stability conditions of the finite difference method are $K\frac{\Delta\tau}{2}+\frac{2\Delta\tau}{(\Delta Y)^2}+S\frac{\Delta\tau}{\Delta Y}\le 1$, $\frac{1}{P_m}\frac{2\Delta\tau}{(\Delta Y)^2}+S\frac{\Delta\tau}{\Delta Y}\le 1$,

$\left(\frac{1+R}{P_r}\right)\frac{2\Delta\tau}{(\Delta Y)^2}+S\frac{\Delta\tau}{\Delta Y}+\beta\bar{T}^{\,p-1}\le 1$ and

$\frac{1}{S_c}\frac{2\Delta\tau}{(\Delta Y)^2}+S\frac{\Delta\tau}{\Delta Y}-\gamma\bar{T}^{\,p-1}\le 1$. When the $\Delta\tau$ and ΔY approach to zero then the problem will be converged. That's mean the results of the finite difference method approach the actual solutions.

VI. RESULTS AND DISCUSSION

For the purpose of discussing the results of the problem, the approximate solutions are obtained for various parameters. To analyze the physical situation of the model, we have computed the steady state numerical solutions. It is also computed the rate of change of the non-dimensional primary velocity *(U)* , secondary velocity *(W)*, primary induced magnetic field *(H_1)*, secondary induced magnetic field *(H_3)*, temperature $(\bar{T})$ and concentration $(\bar{C})$ near the plate within the boundary layer for different values of Suction parameter *(S)*, Permeability of the porous medium *(K)*, α , Magnetic parameter *(M)*, Magnetic diffusivity number (P_m), Hall parameter (β_e), Radiation parameter (R) , Prandtl number (P_r) , Dufour number (D_u), Eckert Number (E_c) , Heat generation or absorption parameter (β) , Schmidt number (S_c) , Soret number (S_r) and Chemical reaction parameter (γ) with the help of a computer programming language Compaq Visual Fortran 6.6a and Tecplot 7. These computed results have been shown graphically. To obtain the steady-state solutions, the computation has been carried out up to $\tau = 80$. It is observed that the numerical values of $U, W, H_1, H_2, \bar{T}$ and $\bar{C}$ however, show little changes after $\tau = 10$. Hence at $\tau = 10$, the solutions of all variables are steady-state solutions.

The importance of cooling problem in nuclear engineering in connection with the cooling of reactors, the value of the Grashof number for heat transfer is taken to be positive and the present study has considered $G_r = 1.00$. Since the most important fluids are atmospheric air and water, so that the results are limited to $P_r = 0.71$ (for air at 20°C) and $P_r = 7.00$ (for water at 20°C). Here the investigation are assumed for both lighter and heavier fluid particles, hence the values of S_c are taken 0.60 and 0.94 (in particular, 0.60 for water vapor that represents a diffusing chemical species of most common interest in air, 0.94 for carbon dioxide) which represent the specific condition of the flow. However the values of another parameters of K , α , M , P_m, β_e, R, D_u , E_c , β , S_r and γ are chosen arbitrarily and also $G_m = 1.00$ for mass transfer are considered as a fixed value. It is noted that $\beta < 0$ and $\beta > 0$ are treated as heat absorption and genaration respectivly. Where $\gamma < 0$ and $\gamma > 0$ are treated as generative and destructive chemical reaction respectively.

To observe the physical situation of the problem, the solutions have been illustrated in Figs. 3-14 when $p = 2$ and $q = 2$. The shear stresses in x-direction have been displayed for various values of K , α , M , P_m, β_e, R , P_r, β , D_u , E_c , S_c , γ , S_r and S respectively illustrated in Figures 3-4. These results show that the shear stress in x -direction decreases with the increase of Permeability of the porous medium, Magnetic parameter, Magnetic diffusivity number, Prandtl number, Schmidt number, Chemical reaction parameter and Suction parameter and opposite effects have been occurred with increase of α , Radiation parameter, Heat generation or absorption parameter, Dufour number, Eckert Number and Soret number. There has no change of shear stress in x -direction with the increase of Hall parameter.

Figures 5-6 show the shear stresses in z -direction for various values of K , α , M , P_m, β_e, R , P_r, β , D_u , E_c , S_c , γ , S_r and S respectively. It has been observed, the shear stress in z -direction of the fluid decreases with the increase of Permeability of the porous medium, α , Magnetic diffusivity number, Prandtl number, Schmidt number, Chemical reaction parameter and Suction parameter and opposite effects have been occurred with increase of Magnetic parameter, Hall parameter, Heat generation or absorption parameter, Dufour number, Eckert Number and Soret number. There has no change of shear stress in z -direction with the increase of Radiation parameter.

The current densities in x -direction have been displayed for various values of K , α , M , P_m, β_e and R respectively illustrated in Figure 7. These results show that current density in x -direction decreases with the increase of Hall parameter and increases with the increase of α , Magnetic parameter and Magnetic diffusivity number. The current density in x -direction slightly decreases with the increase of Permeability of the porous medium. It has been seen the current density in x -direction has no effects with the increase of Radiation parameter.

Figure 8 shows the current densities in z -direction for various values of K , α , M , P_m, β_e and R respectively. These results show that the current density in z -direction slightly decreases with the increase of Permeability of the porous medium. It also decreases with the increase of Magnetic parameter, Magnetic diffusivity number and Hall parameter and opposite effects have been occurred with the increase of α . No effects on current density in z -direction has been found with the increase of Radiation parameter.

Figures 9-10 display the Nusselt numbers for various values of Permeability of the porous medium *(K)*, α, Magnetic parameter (M), Magnetic diffusivity number (P_m), Hall parameter (β_e), Radiation parameter (R), Prandtl number (P_r), Heat generation or absorption parameter (β), Dufour number (D_u), Eckert Number (E_c), Schmidt number (S_c), Chemical reaction parameter (γ), Soret number (S_r) and Suction parameter (S) respectively. These results show that the Nusselt number decreases with the increase of Permeability of the porous medium, Magnetic parameter, Radiation parameter, Heat generation or absorption parameter, Dufour number, Eckert number, Schmidt number and Chemical reaction parameter and increases with the increase of Prandtl number, Soret number and Suction parameter. There has no change of Nusselt number with the increase of α, Magnetic diffusivity number, Hall parameter.

Figures 11-12 show the fluid Sherwood number for several values of Permeability of the porous medium (K), (α), Magnetic parameter (M), Magnetic diffusivity number (P_m), Hall parameter (β_e), Radiation parameter (R), Prandtl number (P_r), Heat generation or absorption parameter (β), Dufour number (D_u), Eckert Number (E_c), Schmidt number (S_c), Chemical reaction parameter (γ), Soret number (S_r) and Suction parameter (S) respectively. The Sherwood number increases with the increase of Permeability of the porous medium, Magnetic parameter, Radiation parameter, Heat generation or absorption parameter, Dufour number, Eckert Number, Schmidt number, Chemical reaction parameter and Suction parameter while decreases with the increase of Prandtl number and Soret number. There have no effects on the Sherwood number with the increase of α, Magnetic diffusivity number and Hall parameter.

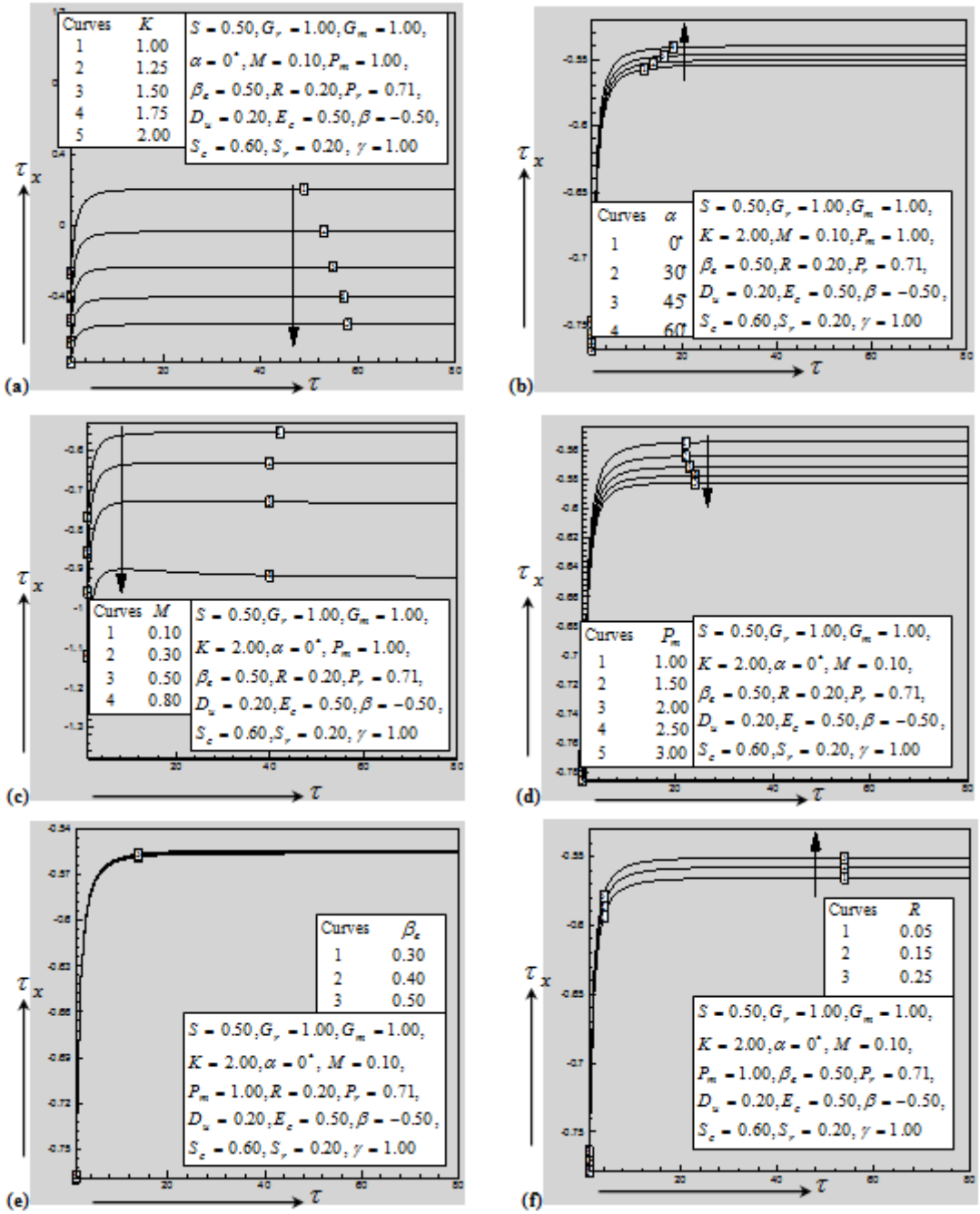

Figure 3. Illustration of shear stress in x-direction for various values of (a) Permeability of the porous medium *(K)*, (b) *(α)*, (c) Magnetic parameter *(M)*, (d) Magnetic diffusivity number *(P_m)*, (e) Hall current parameter *(β_e)* and (f) Radiation parameter *(R)* when *p=2* and q=2.

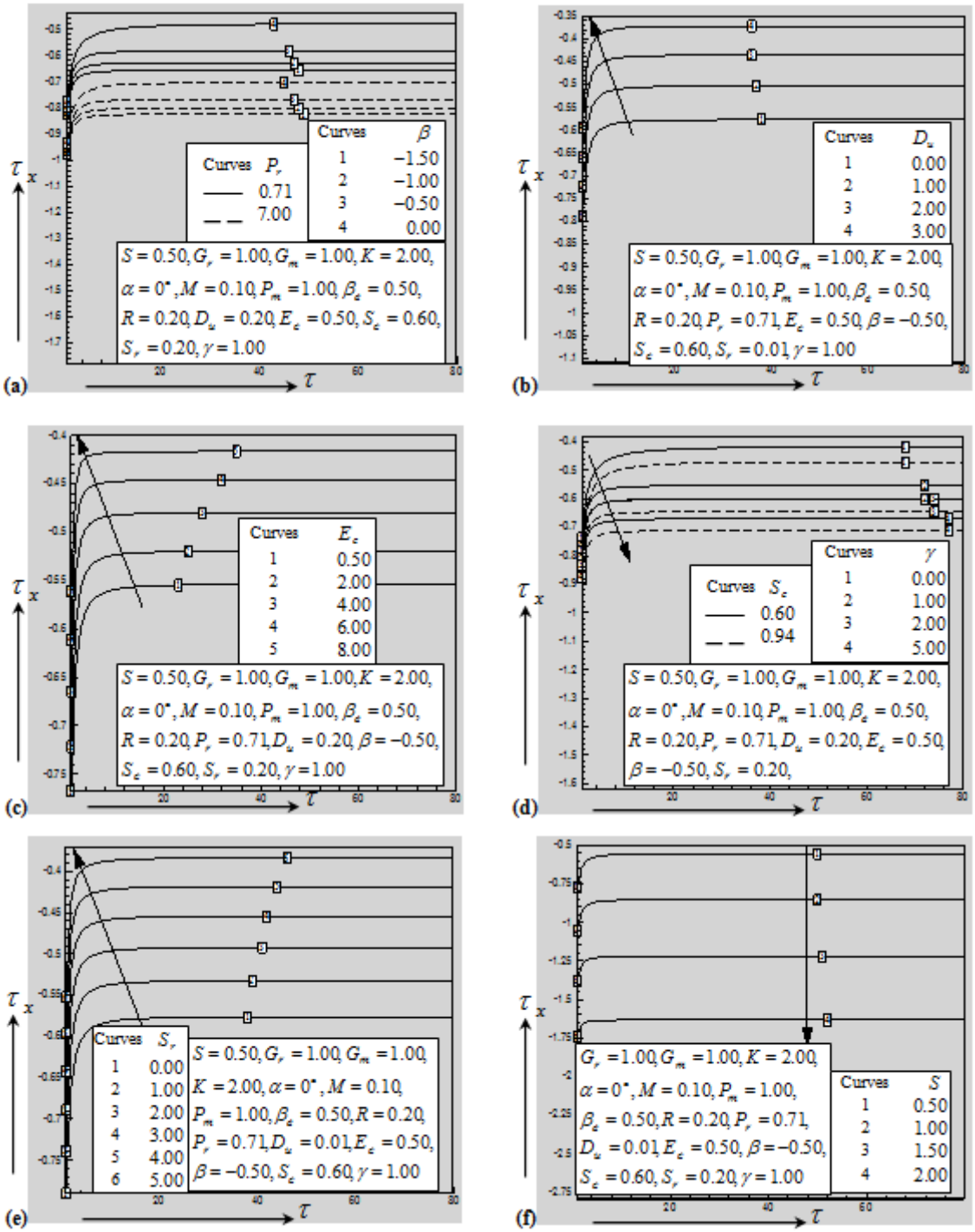

Figure 4. Illustration shear stress in x-direction for various values of (a) Prandtl number (P_r) and Heat genaration or absrption parameter (β), (b) Dufour number (D_u), (c) Eckert number (E_c), (d) Schmidt number (S_c) and Chemical reaction parameter (γ), (e) Soret number (S_r) and (f) Suction parameter (S) when $p = 2$ and $q = 2$.

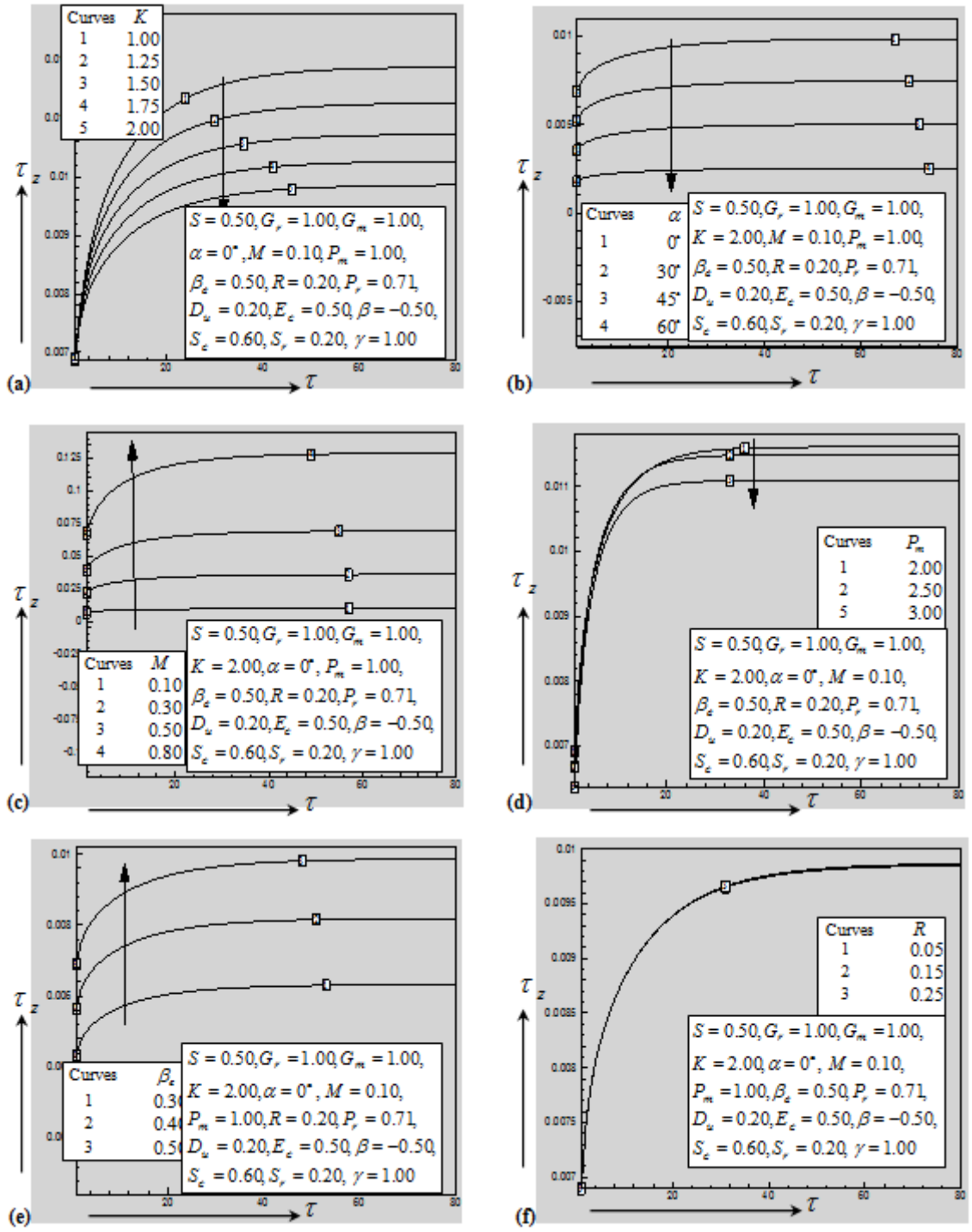

Figure 5. Illustration of shear stress in z-direction for various values of (a) Permeability of the porous medium (K), (b) (α), (c) Magnetic parameter (M), (d) Magnetic diffusivity number (P_m), (e) Hall current parameter (β_e) and (f) Radiation parameter (R) when $p = 2$ and $q = 2$.

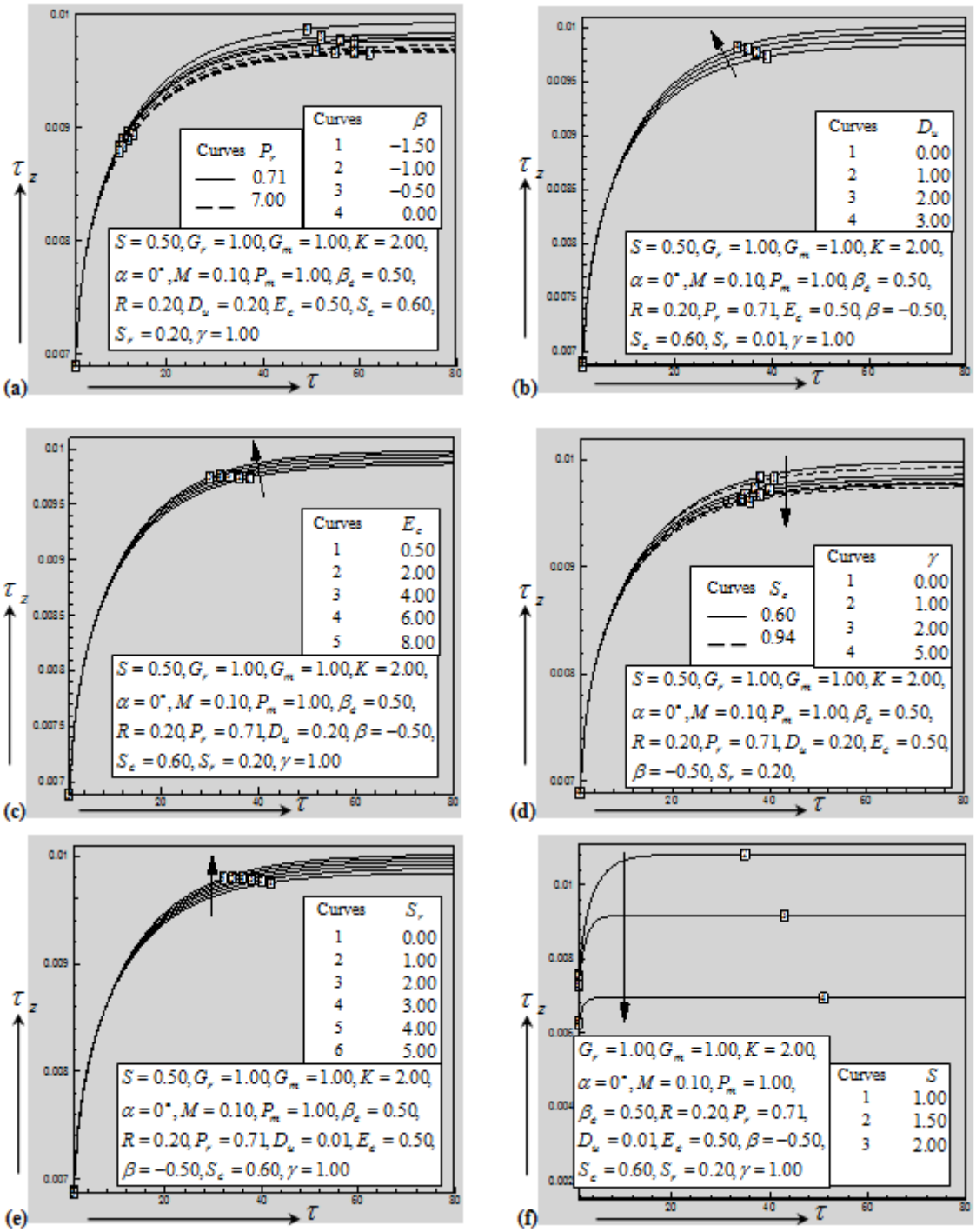

Figure 6. Illustration of shear stress in z -direction for various values of **(a)** Prandtl number (P_r) and Heat genaration or absrption parameter (β), **(b)** Dufour number (D_u), **(c)** Eckert number (E_c), **(d)** Schmidt number (S_c) and Chemical reaction parameter (γ), **(e)** Soret number (S_r) and **(f)** Suction parameter (S) when $p = 2$ and $q = 2$.

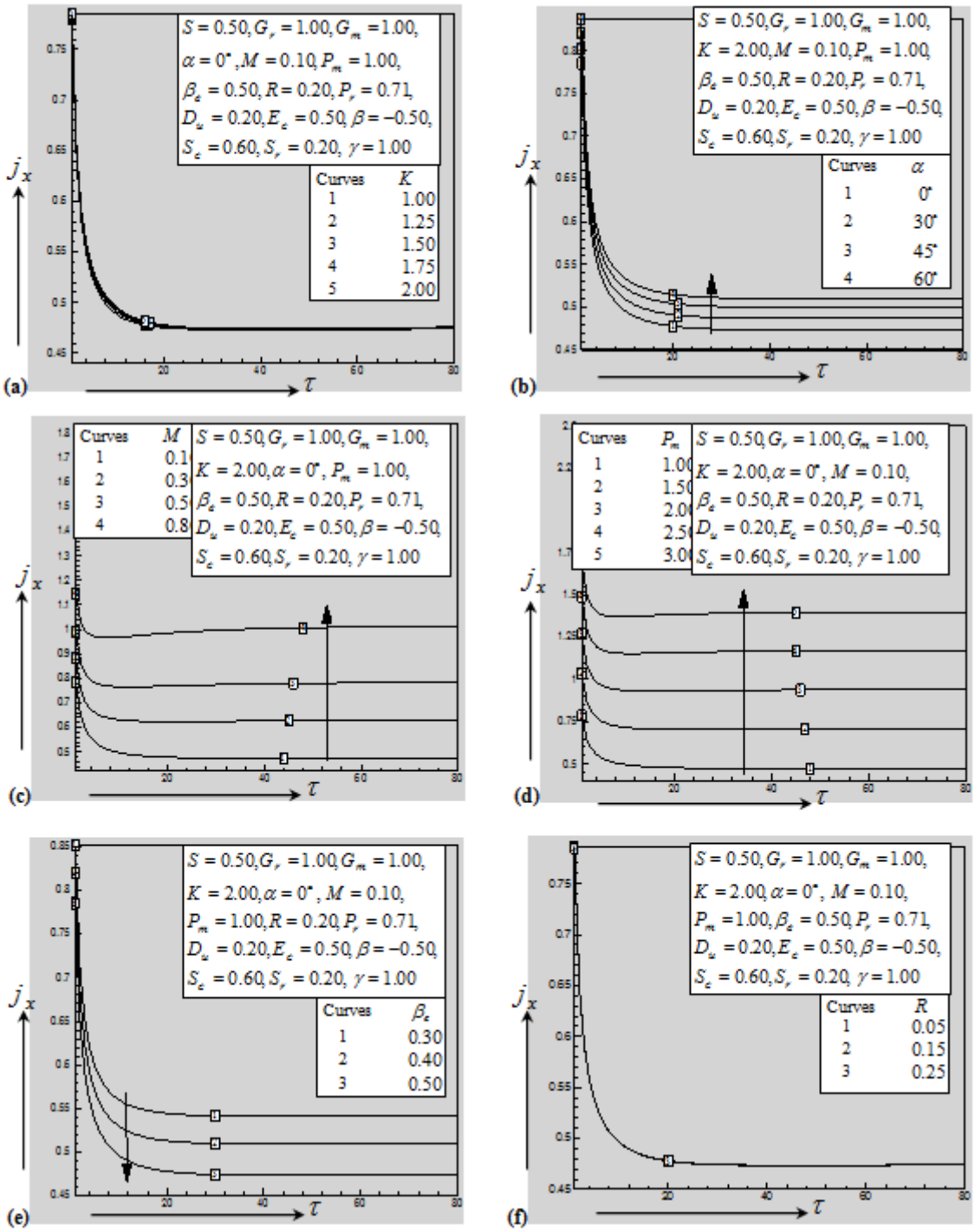

Figure 7. Illustration of current density in x-direction for various values of **(a)** Permeability of the porous medium (K), **(b)** (α), **(c)** Magnetic parameter (M), **(d)** Magnetic diffusivity number (P_m), **(e)** Hall current parameter (β_e) and **(f)** Radiation parameter (R) when $p = 2$ and $q = 2$.

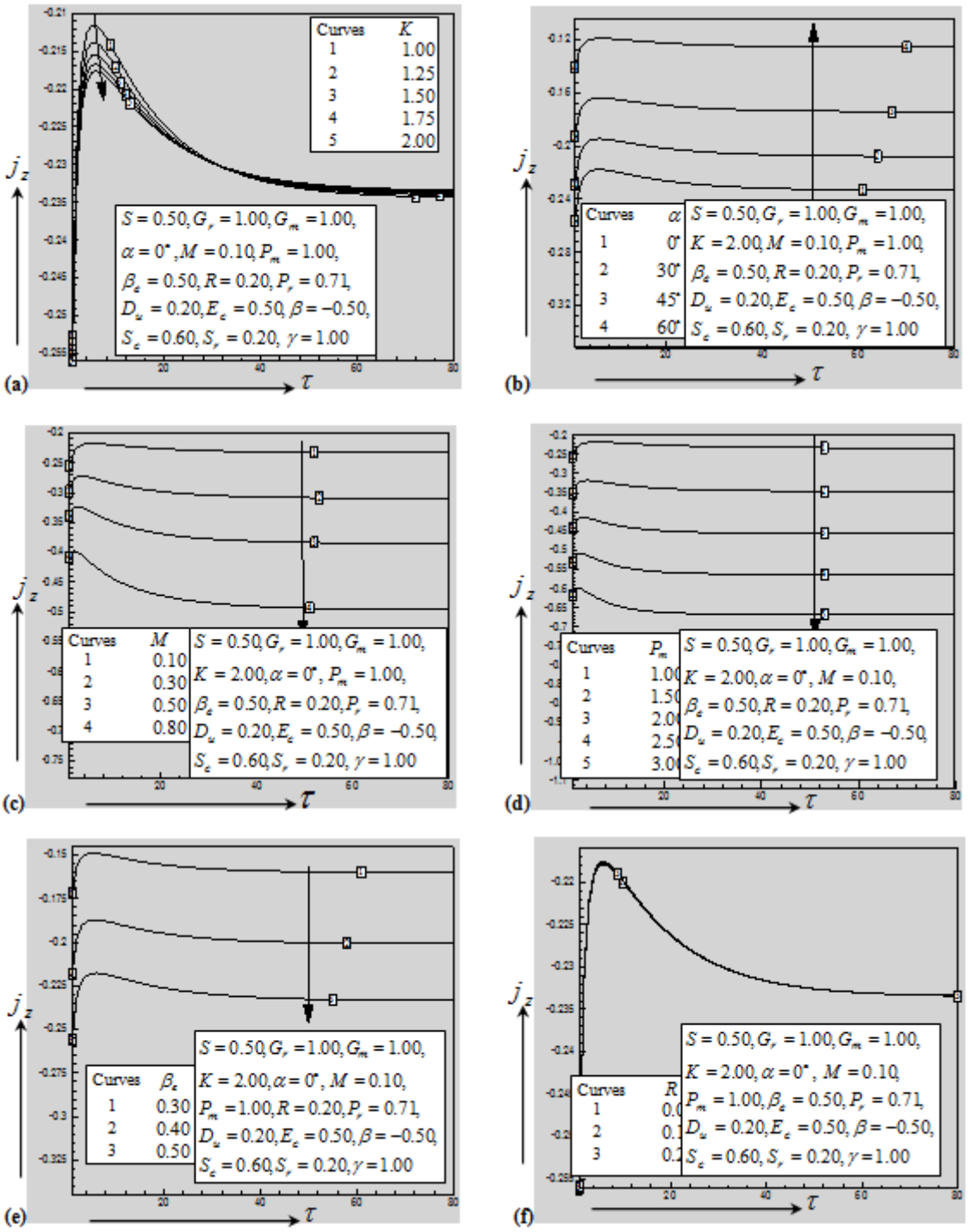

Figure 8. Illustration of current density in z -direction for various values of **(a)** Permeability of the porous medium (K), **(b)** (α), **(c)** Magnetic parameter (M), **(d)** Magnetic diffusivity number (P_m), **(e)** Hall current parameter (β_e) and **(f)** Radiation parameter (R) when $p = 2$ and $q = 2$.

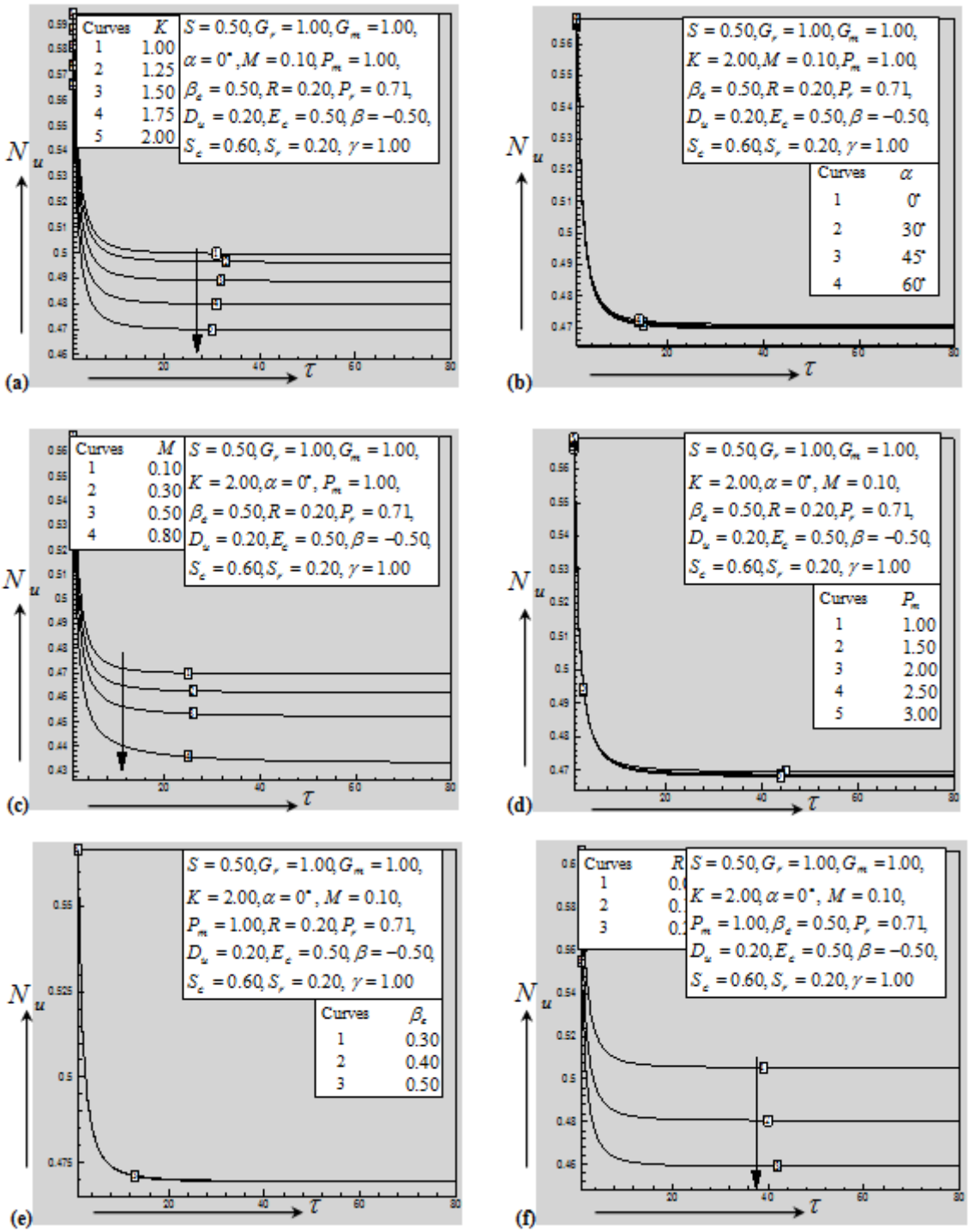

Figure 9. Illustration of Nusselt number for various values of **(a)** Permeability of the porous medium (K), **(b)** α, **(c)** Magnetic parameter (M), **(d)** Magnetic diffusivity number (P_m), **(e)** Hall current parameter (β_e) and **(f)** Radiation parameter (R) when $p = 2$ and $q = 2$.

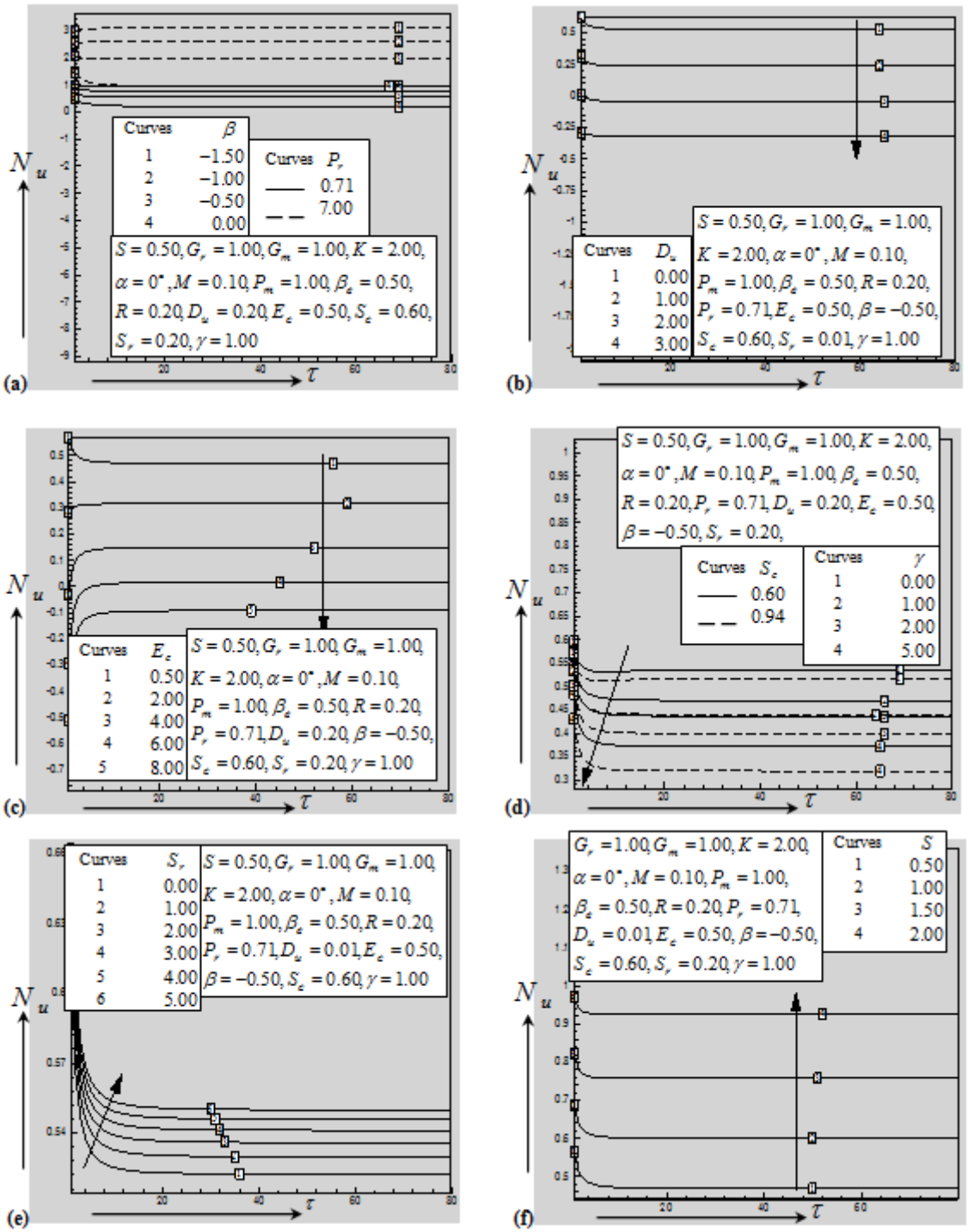

Figure 10. Illustration of Nusselt number for various values of **(a)** Prandtl number (P_r) and Heat genaration or absrption parameter (β), **(b)** Dufour number (D_u), **(c)** Eckert number (E_c), **(d)** Schmidt number (S_c) and Chemical reaction parameter (γ), **(e)** Soret number (S_r) and **(f)** Suction parameter (S) when $p = 2$ and $q = 2$.

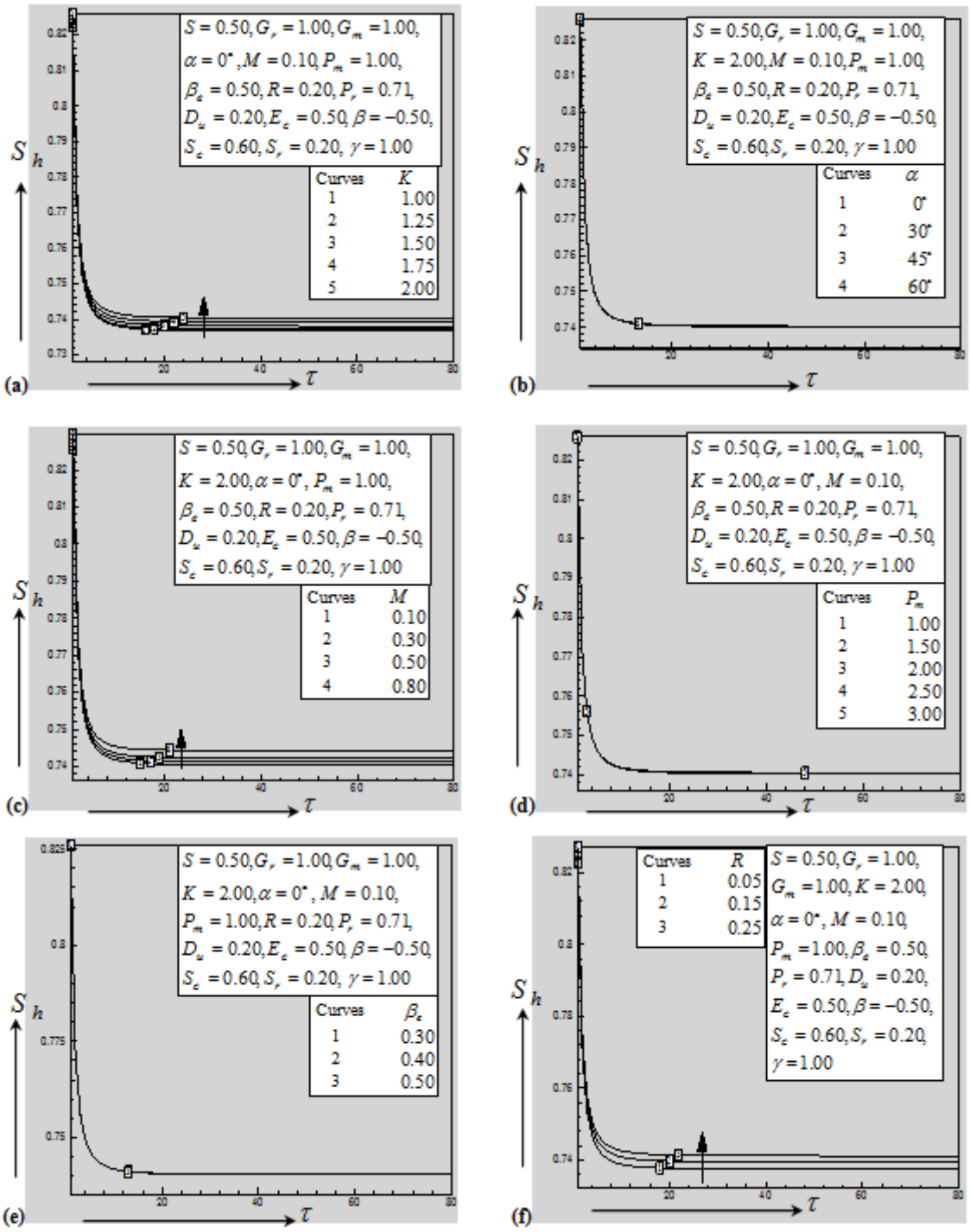

Figure 11. Illustration of Sherwood number for various values of **(a)** Permeability of the porous medium (K), **(b)** α, **(c)** Magnetic parameter (M), **(d)** Magnetic diffusivity number (P_m), **(e)** Hall current parameter (β_e) and **(f)** Radiation parameter (R) when $p = 2$ and $q = 2$.

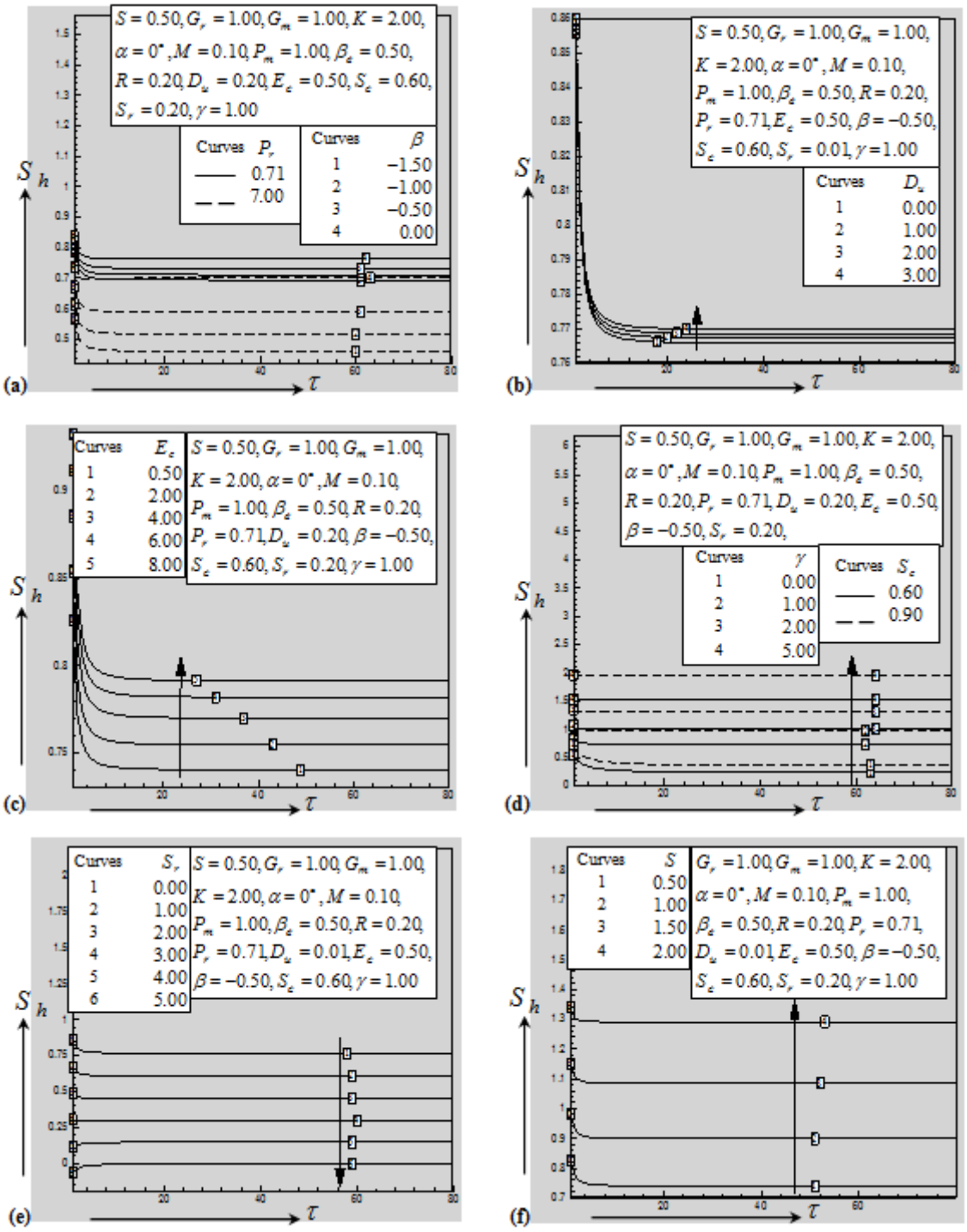

Figure 12. Illustration of Sherwood number for various values of **(a)** Prandtl number (P_r) and Heat genaration or absrption parameter (β), **(b)** Dufour number (D_u), **(c)** Eckert number (E_c), **(d)** Schmidt number (S_c) and Chemical reaction parameter (γ), **(e)** Soret number (S_r) and **(f)** Suction parameter (S) when $p = 2$ and $q = 2$

VII. CONCLUSIONS

The implicit finite difference solution for considerable magnetic Reynolds number of unsteady chemically reacting radiative ionized fluid flow through an impulsively vertical porous plate in the presence of heat generation, joule heating and viscous dissipation for $p \leq 2$ and $q \leq 2$ has been investigated. The physical properties are graphically discussed for different values of corresponding parameters and compared our steady-state results with Haque et al. [15]. The accuracy of our results is qualitatively good in case of all the flow parameters. Some important findings of this investigation are listed below;

1. The shear stress in x-direction decreases with the increase of Permeability of the porous medium, Magnetic parameter, Magnetic diffusivity number, Prandtl number, Schmidt number, Chemical reaction parameter and Suction parameter while increases with the increase of α, Radiation parameter, Heat genaration or absorption parameter, Dufour number, Eckert number and Soret number.
2. The shear stress in z-direction decreases with the increase of Permeability of the porous medium, α, Magnetic diffusivity number, Prandtl number, Schmidt number, Chemical reaction parameter and Suction parameter while increases with the increase of Magnetic parameter, Hall parameter, Heat genaration or absorption parameter, Dufour number, Eckert number and Soret number.
3. The current density x-direction increases with the increase of α, Magnetic parameter and Magnetic diffusivity number while decreases with the increase of Hall parameter.
4. The current density z-direction decreases with the increase of Permeability of the porous medium, Magnetic parameter, Magnetic diffusivity Number and Hall parameter while increases with the increase of α.
5. The Nusselt number decreases with the increase of Permeability of the porous medium, Magnetic number, Radiation parameter, Dufour number, Heat genaration or absorption parameter, Eckert number, Schmidt number, Chemical reaction parameter while increases with the increse of Prandtl number, Soret number and Suction parameter.
6. The Sherwood number decreases with the increase of Prandtl number and Soret number while increases with the increse of Permeability of the porous medium, Magnetic number, Radiation parameter, Dufour number, Heat genaration or absorption parameter, Eckert number, Schmidt number, Chemical reaction parameter and Suction parameter.

As the basis for many scientific and engineering applications for studying more complex problems involving the flow of chemically reacting fluids, it is hoped that the findings of the present study may be useful for study of movement of oil or gas and water through the reservoir of an oil or gas field. The results of the problem are also of great interest in geophysics and astrophysics in the study of interaction of the geomagnetic field with the fluid in geothermal region.

NOMENCLATURE

x, y and z	Cartesians co-ordinates in the three directions
U_∞	Constant velocity of plate movement
T_w, C_w	Temperature and spices concentration at the wall
T_∞, C_∞	Temperature and concentration of the species outside the plate
t	Time
H_0	Imposed uniform magnetic field
α	Uniform magnetic field H_0 applied in a direction that makes an angle with the normal to the considered plate
H	The resultant magnetic field vector
J	The current density vector
J_x, J_y and J_z	Current densities in the three directions
u, v and w	Velocities in the three directions
v_0	The suction velocity
H_x, H_y and H_z	Components of magnetic induction vector in the three directions
H_w	The magnetic induction at the wall
g	Local acceleration due to gravity
β_T	The thermal expansion coefficient
β_C	The concentration expansion coefficient
υ	The kinematic coefficient viscosity
μ	The fluid viscosity
μ_e	The magnetic permeability
ρ	The density of the fluid
κ	The thermal conductivity
c_p	The specific heat at the constant pressure
k_0	The rate of chemical reaction
D	The coefficient of mass diffusivity

k_t	The thermal diffusion ratio
c_s	The concentration susceptibility
p , q	positive constants
q_r	The radiative heat flux
σ^*	The Stefan-Boltzman constant
k^*	The mean absorption coefficient
τ	The dimensionless time
Y	The dimensionless Cartesian coordinate in *y*-direction
U and W	The dimensionless velocity components in *x* and *y* directions
H_1 and H_2	The dimensionless primary and secondary induced magnetic field
$\overline{T}$	The dimensionless temperature
$\overline{C}$	The dimensionless concentration
S	Suction Parameter
G_r	Grashof Number
G_m	Modified Grashof Number
K	Permeability of the porous medium
M	Magnetic Parameter
P_m	Magnetic diffusivity Number
R	Radiation Parameter
P_r	Prandtl Number
D_u	Dufour Number
E_c	Eckert Number
β	Heat Generation or Absorption Parameter
S_c	Schmidt Number
S_r	Soret Number
γ	Chemical Reaction Parameter
τ_x	Shear stress in *x*-direction
τ_z	Shear stress in *z*-direction
J_x	Current density in x-direction
J_z	Current density in *z*-direction
N_u	Nusselt number
S_h	Sherwood number
$Y_{\max}$	The maximum length of boundary layer

REFERENCES

[1] T. G.Cowling , Magnetohydrodynamics, Interscience Publications, New York (1957).

[2] P. C. Ram , *Astrophysics and Space Science*, 149, 171 (1988).

[3] B. P. Garg, International Journal of Pure and Applied Mathematics, 81, 335 (2012).

[4] DAMSEH Rebhi , H. M. DUWAIRI and M. AL-ODAT , *Turkish J. Eng. Env. Sci.*, 30, 83 (2006).

[5] M. A. Samad and M.M. Rahman, Journal of Naval Architecture and Marine Engineering, 3, 7 (2006).

[6] U. N. Das, R. Dekha and V. M. Soungalgekar, *Forschungim Ingenieurwesen*, 60, 284 (1994).

[7] O. D. Makinde , *Chemical Engineering Communications*, 198, 590 (2010).

[8] N. G. Kafoussias and E. W. Williams, *International Journal of Engineering Science*, 33, 1369 (1995).

[9] A. Postelnicu, International Journal of Heat and Mass Transfer, 47, 1467, (2004).

[10] S. Shateyi , S. S. Mosta and P. Sibanda, *Mathematical Problems in Engineering*, Article ID 627475 (2010).

[11] P. O. Olanrewaju and J. A. Gbadeyan , *Pacific Journal of Science and Technology*, 11, 1 (2010).

[12] Aurangzaib, and S. Shafie, Canadian Journal on Science and Engineering Mathematics, 2, 153 (2011).

[13] T. Ahmed and M. M. Alam, *Proceedia Engineering*, 56, 149 (2013).

[14] M. M. Alam , M. R. Islam , M. Wahiduzzaman and F. Rahman, *Journal of Energy Heat and Mass Transfer*, 34, 193 (2012).

[15] M. M. Haque , M. M. Alam ,M. Ferdows and Q. M. Al-Mdallal, *International Journal of Applied Electromagnetic and Mechanics*, 41, 121 (2013).

[16] B. Carnahan , H.A. Luther and J. O. Wilkes, *Applied Numerical Methods, John Wiley & Sons*, New York (1969).

[17] M. Q. Brewster , Thermal Radiative Transfer and Properties, John Wiley and Sons Inc., New York: USA (1992).

How to Cite this Article:

Ahmed, T., Alam, M., Bangalee, M. Z. I., Ferdows, M. & Quadir, R. A. (2019) Chemically Reacting Ionized Fluid Flow through a Porous Medium along an Impulsively Started Permeable Vertical Plate with Induced Magnetic Field and Viscous Dissipation. International Journal of Science and Engineering Investigations (IJSEI), 8(92), 17-34. http://www.ijsei.com/papers/ijsei-89219-03.pdf